Advanced Powder Technology xxx (2017) xxx–xxx

Contents lists available at ScienceDirect

Advanced Powder Technology

journal homepage: www.elsevier.com/locate/apt

Original Research Paper

Effect of Fe doping on the structural, optical and magnetic properties of combustion synthesized nanocrystalline ZnO particles

N. Srinatha [a], K.G.M. Nair [b], Basavaraj Angadi [a,*]

[a] Department of Physics, JB Campus, Bangalore University, Bangalore 560056, India
[b] UGC-DAE-CSR, Kalpakkam Node, Kalpakkam, Kokilamedu 603 102, India

ARTICLE INFO

Article history:
Received 7 February 2016
Received in revised form 13 November 2016
Accepted 18 January 2017
Available online xxxx

Keywords:
ZnO
L-Valine
Room temperature ferromagnetism
Electron microscopy
Band gap energy

ABSTRACT

In the present study, the effect of Fe substitution in nanocrystalline $Zn_{1-x}Fe_xO$ (x = 0, 0.01, 0.03, 0.05 and 0.07) particles synthesized through solution combustion are reported. The detailed structural and microstructural studies of as-synthesized samples were carried out through X-ray Diffraction (XRD), Scanning Electron Microscopy (SEM) and Transmission Electron Microscopy (TEM). Further, the optical and magnetic properties were investigated respectively through Diffuse Reflectance Spectroscopy and Superconducting Quantum Interference Device (SQUID). The XRD results as well as the Rietveld refinement on XRD data reveals the single phase, polycrystalline nature of the prepared materials and no impurities such as $ZnFe_2O_4$, Fe_2O_3, Fe_3O_4 were seen, which confirms the substitution of Fe at Zn site. SEM and TEM studies reveal that, the samples are porous and agglomerated due to the evolution of large amount of gases during the combustion and also as-formed particles are found to be in nano-range with an particle size varies from 20 to 25 nm. Optical studies show that, the absorption edge shifts to lower energy/higher wavelength. Room temperature magnetic (SQUID) studies shows that the undoped ZnO exhibit diamagnetic property where as Fe doped ZnO exhibit intrinsic room temperature ferromagnetism (RTFM) with increasing coercivity with Fe concentration and is attributed to the incorporation of Fe into ZnO host matrix.

1. Introduction

Recently, diluted magnetic semiconductors (DMSs), such as Fe doped ZnO, are receiving more attention as the potential candidates for information storage and processing devices in the field of spintronics, opto-electronics, magneto-electronics and micro-electronics industry [1–3] due to their tunable semiconducting (optical band gap) and magnetic (ferromagnetism) properties at room temperature. The substitution of transition metals such as Fe, Co, and Ni in the host ZnO would lead into the change in the band gap energy. In fact, the tunability of the band gap of ZnO nanoparticles upon doping Fe, Co, etc. is important for the desired applications in various opto-electronics devices. In particular, in the case of Fe-doped, there is a large variability in the optical behavior and that leads to inconsistent conclusions [4,5]. In addition, existence of room temperature ferromagnetism (RTFM) is sensitive to the synthesis methods and synthesis conditions [4–16]. Till date, there are several methods have been reported to synthesize the transition metal (Fe) doped ZnO, such as co-precipitation [5], spray pyrolysis [6], sol-gel [7], and solution combustion [8]. There also controversial reports on the existence of ferromagnetism (FM) at room temperature (RT), that it might come from the presence of magnetic clusters or secondary phases [9] and few other reports claiming, defects plays a crucial role in the existence of RTFM in the undoped as well as in the transition metal doped ZnO [10]. In literature, till date the existence of RTFM in transition metal doped ZnO has been reported in thin films [6,11] and nanoparticles [5–8,12,13], whereas some other groups have reported an absence of RTFM [14,15]. In particular, there are reports [13,16] which show that, RTFM was observed for the lower concentration of Fe (<4%) and at higher Fe doping concentrations as the ferromagnetic property (coercivity) suppressed by the paramag netic/antiferromagnetic property in Fe doped ZnO nanoparticles. Hence, the origin of ferromagnetism in ZnO-based DMSs remains as a very controversial topic and still under debate. In view of this, in the present study, we have synthesized undoped and Fe doped ZnO nanoparticles through solution combustion technique using new fuel, L-Valine for the first time. Further, the effect of Fe substi-

* Corresponding author.
E-mail address: brangadi@gmail.com (B. Angadi).

http://dx.doi.org/10.1016/j.apt.2017.01.016
0921-8831/

tution on the structural, optical and magnetic properties are investigated and discussed in detail.

2. Experimental

Nanocrystalline $Zn_{1-x}Fe_xO$ ($x = 0$, 0.01, 0.03, 0.05 and 0.07) particles were synthesized through solution combustion technique using Zinc Nitrate Hexa-hydrate ($Zn(NO_3)_2{\cdot}6H_2O$) as an oxidizer, Ferrous Nitrate nonahydrate ($Fe(NO_3)_3{\cdot}9H_2O$) as dopant and L-Valine ($C_5H_{11}NO_2$) as a fuel for the first time. All the chemicals were AR grade (SD fine Chemicals, India) and were used directly without purification. The stoichiometric balanced equation used is as follows;

$$27(1-x)\ Zn(NO_3)_2\cdot 6H_2O + 2x\ Fe(NO_3)_3\cdot 9H_2O + (10+8x)C_5H_{11}NO_2 + \left(\frac{27}{2}x\right)O_2 \rightarrow 27Zn_{1-x}Co_xO + 5(10+8x)CO_2\uparrow + \left(\frac{64+35x}{2}\right)N_2\uparrow + (217+125x)\ H_2O\ \uparrow \quad (1)$$

Stoichiometric amounts of precursors were taken based on the condition that the sum of the valances of O/F ratio to be unity, using total oxidizing and reducing valences of the precursors. These stoichiometric amounts of precursors were dissolved in double distilled water and stirred thoroughly until to get transparent, homogeneous solution called redox mixture. The redox mixture was dried in muffle furnace at 100 °C to remove water content. So obtained sticky solution (water free) was then placed in the pre-heated muffle furnace at 400 °C. Within about 5 min, the solution (gel) ignites, fires with flame and finally left with voluminous foamy product (ash). The final foamy product was collected and ground using agate make pestle and mortar.

As-synthesized samples were characterized for phase purity and crystallinity using X-ray Diffractometer (*D8 ADVANCE*, *Bruker*) with wavelength 1.5418 Å. The detailed micro-structural and structural studies were carried out through Field Emission-Scanning Electron Microscopy (FESEM), *SUPRA 55 FESEM/EDX* (*M/s Carl Zeiss*, *Germany*) and High Resolution Transmission Electron Microscopy (HR-TEM) using LIBRA 200 TEM (M/s Carl Zeiss, Germany). Optical properties were investigated through room temperature diffused reflectance spectra recorded in the 200–1600 nm wavelength range using a DRS Spectroscopy Model: JASCO V 670, Japan. The room temperature magnetic properties were investigated through Superconducting Quantum Interference Device (SQUID) magnetometer.

3. Results and discussion

3.1. Structural studies using XRD

XRD patterns of as synthesized $Zn_{1-x}Fe_xO$ ($x = 0$, 0.01, 0.03, 0.05 & 0.07) samples are depicted in Fig. 1(a). From the XRD patterns, all the crystalline peaks are indexed to the JCPDS card no. 36-1451, belongs to hexagonal wurtzite ZnO phase with space group *P63mc*, evidenced that, single phase, polycrystalline nature of pure and Fe doped ZnO samples are obtained at as-synthesis form without need of post annealing steps. It is due to the high exothermicity of the fuel-oxidizer which leads to the formation of single phase, polycrystalline samples. Furthermore to trace presence of impurities, Rietveld refinement has been carried out using FullProf software and the Rietveld fitted patterns are depicted in Fig. 1(b) and the refined lattice parameters and unit cell volume are tabulated in Table 1. From Fig. 1(b), clear observation shows that, no traces of impurities such as $ZnFe_2O_4$, Fe_2O_3, Fe_3O_4 and cluster of metallic Fe are seen. It confirms that, 'Fe' ions are substituted at 'Zn' site without any secondary phase formation. A negligible peak shift has been observed increasing Fe doping could be due to the small doping concentration of Fe (<7%) and also the relative difference in the ionic radii of Fe^{2+} (0.63 Å) and Zn^{2+} (0.60 Å), in tetrahedral coordination is small and considerably negligible, which is evidenced from the negligible variation in the lattice parameters and unit cell volume. However the negligible shift could be due to the micro-strain induced during the combustion synthesis due to the exothermicity of the fuel used.

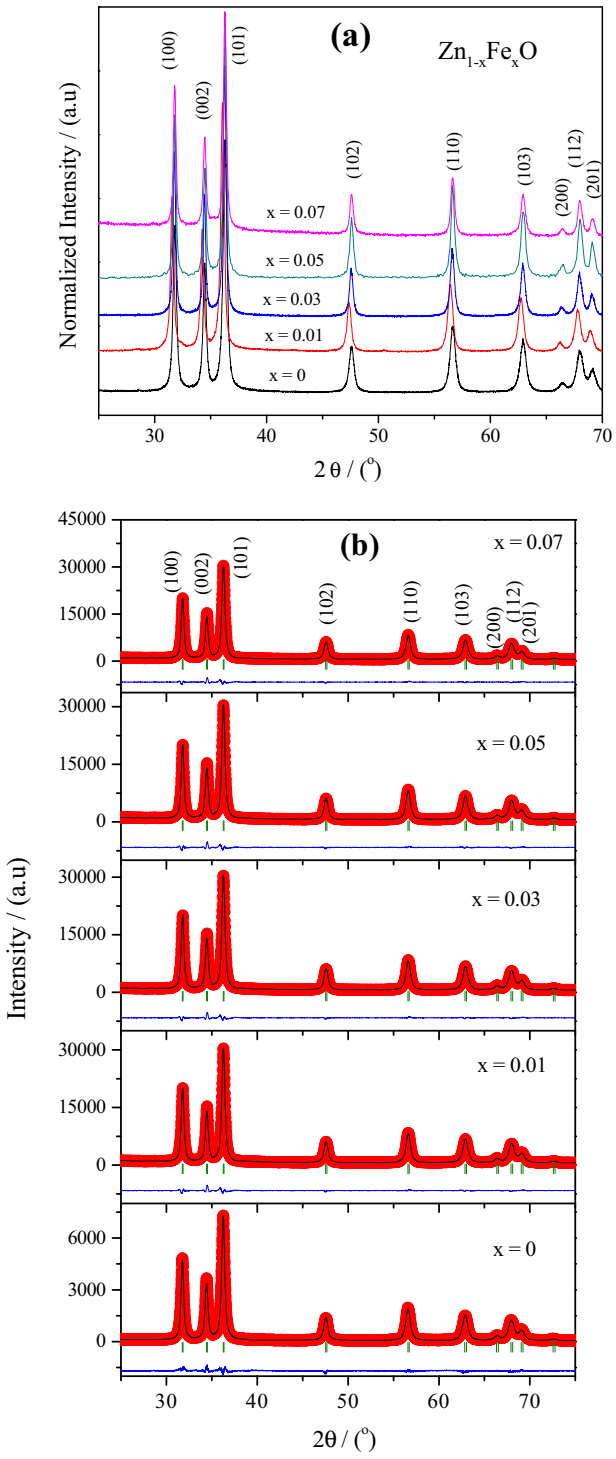

Fig. 1. (a) The PXRD and (b) Rietveld fitted pattern of as synthesized $Zn_{1-x}Fe_xO$ ($x = 0$, 0.01, 0.03, 0.05 and 0.07) samples.

Please cite this article in press as: N. Srinatha et al., Effect of Fe doping on the structural, optical and magnetic properties of combustion synthesized nanocrystalline ZnO particles, Advanced Powder Technology (2017), http://dx.doi.org/10.1016/j.apt.2017.01.016

Table 1
Summary of crystallite size, lattice parameters and energy band gap of $Zn_{1-x}Fe_xO$ for different Fe concentrations.

$Zn_{1-x}Fe_xO$	D_{sh}/(nm)	Lattice parameters		V (Å^3)	(E_g) (eV)
		$a = b$/(Å)	c/(Å)		
$x = 0$	17.5	3.2510 (1)	5.2060 (1)	47.64	3.25
$x = 0.01$	17.8	3.2507 (1)	5.2058 (1)	47.63	3.23
$x = 0.03$	17.9	3.2507 (1)	5.2060 (1)	47.64	3.20
$x = 0.05$	18.0	3.2508 (1)	5.2061 (1)	47.64	3.13
$x = 0.07$	18.1	3.2509 (1)	5.2063 (1)	47.65	3.06

The Crystallite size is calculated using Scherer's formula (2).

$$D = \frac{k\lambda}{\beta \cos\theta} \tag{2}$$

where β is the observed FWHM, θ is the Bragg angle, k is the Scherer's constant, λ is the wavelength of the X-rays used, D is the crystallite size.

The estimated average crystallite sizes are tabulated in Table 1. From the estimated average crystallite sizes, negligible significant variation (increase) in the size of crystallites is observed with Fe concentration may be due to the relative Fe concentration is small in ZnO. It could be attributed to the exothermicity of the redox mixture of fuel-oxidizer precursor and the number of moles of gases evolved during the combustion reaction. That is, the crystallite size of the combustion synthesized material is strongly dependent on the exothermicity of the combustion reaction. In this case the inclusion of Fe precursor along with the Zn precursor would have enhanced the exothermicity of the redox mixture compared to the undoped redox mixture, hence large amount of gases are liberated during the combustion process. As a result, with increase of Fe concentration, the significant increase of crystallite size is observed. It also confirms the substitution of Fe at Zn site without leading to the formation of impurity phases. From the XRD results concludes that, the Fe doping has not produced significant change in the structural parameters tabulated (Table 1), could be due to the low concentration of Fe doping (<7%) and the negligible difference between the ionic size of Fe^{2+} and Zn^{2+} ions.

3.2. Microstructural studies by SEM - EDS and TEM

The surface morphology, composition and micro-structural studies were carried out using Scanning Electron Microscopy (SEM), Energy Dispersive X-ray Spectroscopy (EDS) and Transmission Electron Microscopy (TEM), respectively. The SEM micrographs of undoped and 5% Fe doped ZnO samples are depicted in Fig. 2. It is seen that, the samples are agglomerated with porous nature. These pores and voids are created due to the evolution of large amount of gases which escapes from the material during the combustion process. Clear observation shows that, the particles appear to be spherical within the agglomeration limit. Fig. 2(c) depicts the EDS spectra of 5% Fe doped ZnO sample, which clearly shows the presence of Fe content in ZnO matrix.

TEM micrographs of Fe doped ZnO samples with different Fe content are depicted in Fig. 3. From Fig. 3(a)–(c), left micrographs, the HR-TEM images exhibit clear distinct diffraction rings indicates the high crystalline nature of the material, which is further evidenced from the Inverse Fast Fourier Transformation (IFFT) image obtained from the HRTEM image (top-right image of Fig. 3(a)–(c)), from which the d-spacing was estimated. The estimated d-spacing is found to be ~0.260 nm corresponding to (002) plane. This indicates that large numbers of the crystals/particles are oriented along (002) plane. Further, the down-right image of Fig. 3(a)–(c) and Fig. 3(d) shows the TEM image of Fe doped ZnO samples with different Fe contents (1%, 3%, 5% and 7%), respectively. From which, it is seen that, the particles are agglomerated and the estimated average size of the particles found to be 20–25 nm, which are in agreement with the XRD results.

3.3. UV–visible spectroscopy

Further to investigate the effect of Fe substitution on the optical band gap energy, the optical diffuse reflectance spectra were recorded using UV–Visible diffuse reflectance spectroscopy and are depicted in Fig. 4(a). It is observed from Fig. 4(a) that, the absorption edge of $Zn_{1-x}Fe_xO$ nanoparticles is shifted towards lower energy/higher wavelength (red[1] shifted) with increasing 'Fe' content as compared to the band gap of bulk ZnO (3.37 eV).

The optical band gap of $Zn_{1-x}Fe_xO$ (x = 0, 0.01, 0.03, 0.05 & 0.07) samples are estimated using the diffused reflectance data (Fig. 4(a)). The acquired diffuse reflectance spectrum can be converted to Schuster-Kubelka-Munk function using the formula (3) [17];

$$F(R_\infty) = \frac{(1-R_\infty)^2}{2R_\infty} = \frac{k}{s} \tag{3}$$

where 'k' is the absorption co-efficient, 's' is the scattering co-efficient and 'R_∞' is the Reflectance.

The vertical axis (R_∞) of Fig. 4(a) is converted to quantity $F(R_\infty)$, which is proportional to the absorption coefficient. Hence, the 'α' in the Tauc equation can be replaced with $F(R_\infty)$. Therefore, for direct allowed transition, the Tauc's relation becomes;

$$(h\nu F(R_\infty))^2 = A(h\nu - E_g) \tag{4}$$

The plot of $(h\nu F(R_\infty))^2$ along y-axis vs $h\nu$ along x-axis are depicted in Fig 4(b)–(f). The E_g values are determined by extrapolating the linear region of the $(h\nu F(R_\infty))^2$ vs $h\nu$, that is, the $h\nu$ value of x-axis at $(F(R)h\nu)^2 = 0$ gives the band gap (E_g) and are tabulated in Table 1. It is noteworthy that, the E_g value of the ZnO is 3.25 eV, whereas those of $Zn_{1-x}Fe_xO$ (x = 0.01. 0.03, 0.05 & 0.07) are 3.23, 3.20, 3.13 and 3.06 eV, respectively. Therefore, the estimated E_g of $Zn_{1-x}Fe_xO$ decreases with increase in the Fe concentration. Similar behavior has been reported by Saleh et al. [6] and this red shift of band gap was explained on the basis of a variation of the lattice parameters due to the effect of doping. In our results, we have not seen much variation of lattice parameters since the concentration of Fe doping is relatively small (<7%). Few reports [18,19] also shows the similar trend that the red shift or decrease in band gap to the formation of new molecular orbitals of TM (Mn, Cr) and to the transition between partially forbidden valence band to conduction band. Whereas, Kumar et al. [20] attributed to the incorporation of Co into ZnO due to the sp - d exchange interaction between the localized d electrons of the Co ions. Therefore in the present case, we observed that, the increase of particle size with Fe doping due to the substitution of larger ionic size of Fe^{2+} ions at Zn^{2+} site as a result the band gap energy decreases. This red shift confirms the substitution of Fe^{2+} ions at Zn^{2+} site without formation of impurities in the host matrix. When Fe^{2+} ions enter lattice

[1] For interpretation of color in Fig. 4, the reader is referred to the web version of this article.

Please cite this article in press as: N. Srinatha et al., Effect of Fe doping on the structural, optical and magnetic properties of combustion synthesized nanocrystalline ZnO particles, Advanced Powder Technology (2017), http://dx.doi.org/10.1016/j.apt.2017.01.016

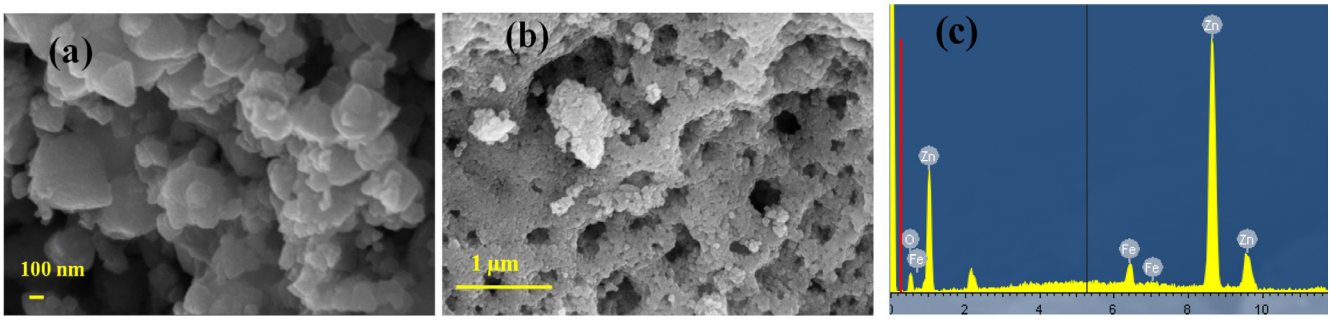

Fig. 2. SEM micrograph of (a) undoped and (b) 5% Fe doped ZnO samples, respectively. (c) EDS spectra of 5% Fe doped ZnO sample.

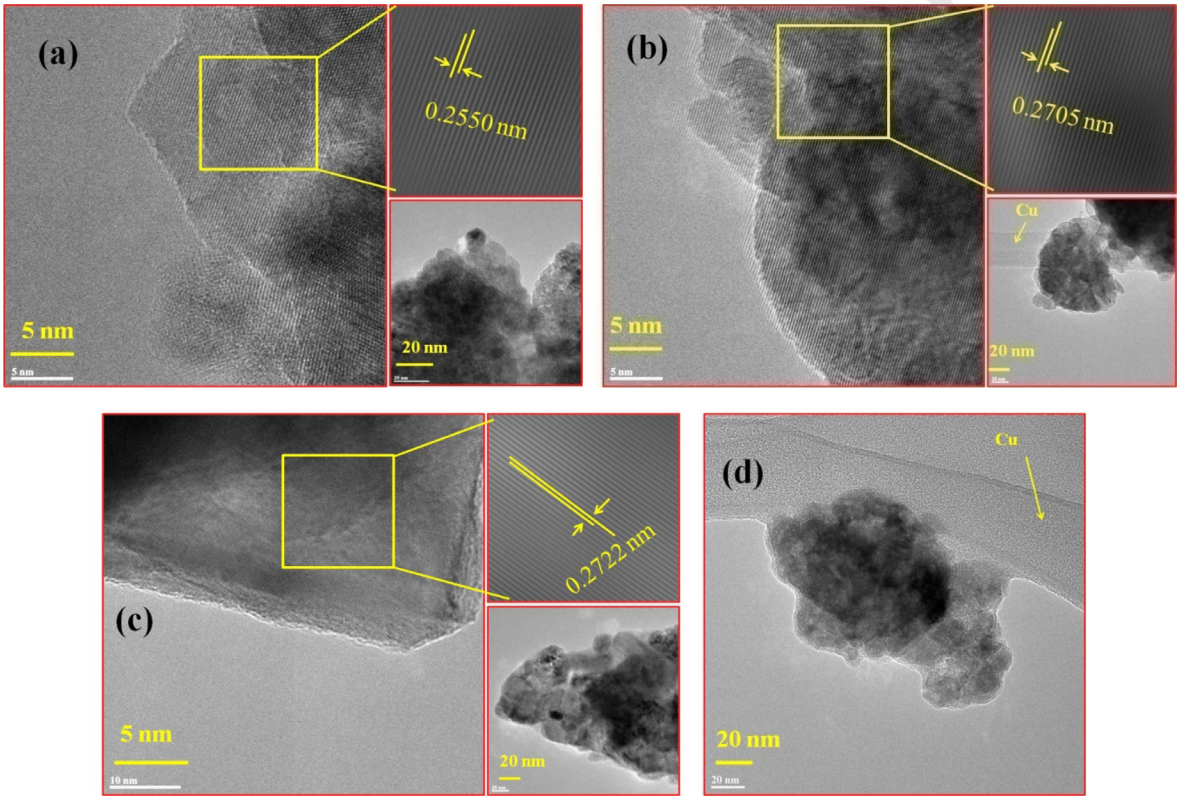

Fig. 3. TEM micrographs of (a) 1%, (b) 3%, (c) 5% and (d) 7% Fe doped ZnO samples.

sites previously occupied by Zn^{2+} ions, they provide additional bands/sub-bands just below the conduction band. These sub-bands merge with conduction band forming continuous band leading to the reduction of band gap. Also, this red shift of band gap is attributed to the *sp – d* exchange interactions between the localized *d* orbit electrons of Fe^{2+} and the band electrons of the ZnO [20].

3.4. Magnetic properties by SQUID magnetometer

Room temperature magnetic properties were investigated through Superconducting Quantum Interference Device (SQUID) magnetometer. Fig. 5 shows the M-H loops for $Zn_{1-x}Fe_xO$ (x = 0.01, 0.05 & 0.07) samples at room temperature after subtracting the paramagnetic component from it. The undoped ZnO sample show noticeable opening of M-H loop could be due to the presence of oxygen vacancies or some other defects being introduced during combustion synthesis, which is evidenced form our earlier reports [12]. However, the slope of the M-H curve is found to be negative indicating the diamagnetic nature (left-top inset) of undoped ZnO. Further, with the incorporation of magnetic Fe in ZnO host, a clear hysteresis with noticeable coercivity was observed (bottom-down inset). With increase of Fe concentration, the area of the loop increases i.e. the remnant magnetization and coercivity increases. Clear hysteresis loops with the coercivity 7.0, 7.25, 8.2 and 8.8 mT were observed for 1%, 3%, 5% and 7% Fe doped ZnO samples, respectively. Their corresponding remnant magnetizations are 0.263×10^{-3}, 0.286×10^{-3}, 2.203×10^{-3} and 9.815×10^{-3} emu/g and the saturation magnetizations are 0.0028, 0.0033, 0.026 and 0.093 emu/g, respectively. The noticeable coercivity of Fe doped ZnO samples is attributed to the existence of ferromagnetism (FM) at room temperature (RT) which arises due to the substitution of ferromagnetic Fe into ZnO host lattice. Also it is seen that, the remnant and saturation magnetization increases with Fe concentration. Till today, the origin of RTFM in such DMS materials is not known clearly and still under debate. However, the origin of ferromagnetic property can be attributed to the following; (i) the exchange interaction between the free delocalized carriers (hole

Please cite this article in press as: N. Srinatha et al., Effect of Fe doping on the structural, optical and magnetic properties of combustion synthesized nanocrystalline ZnO particles, Advanced Powder Technology (2017), http://dx.doi.org/10.1016/j.apt.2017.01.016

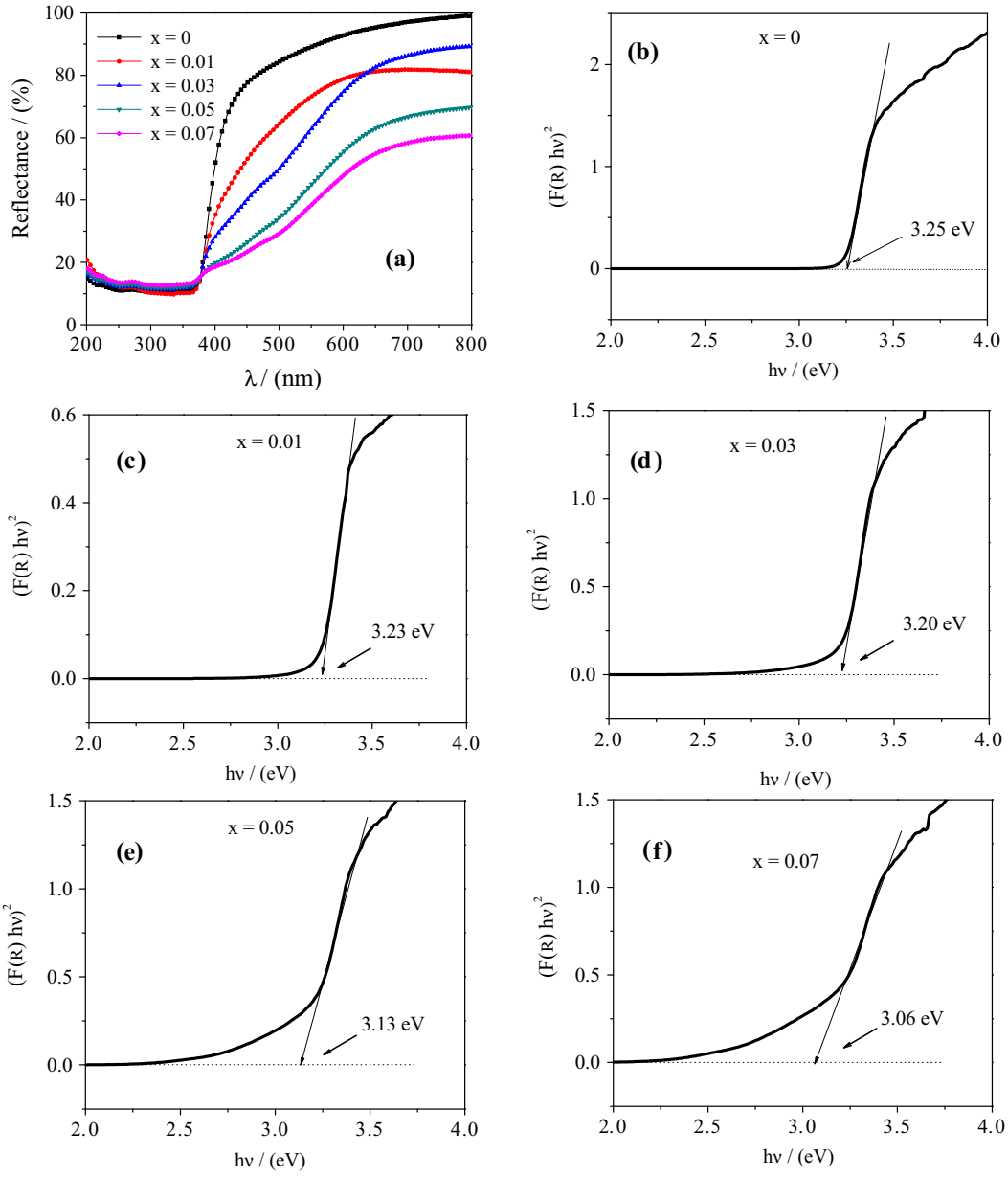

Fig. 4. (a) Diffuse reflectance spectra and (b-f) plots of $(h\nu F(R_\infty))^2$ – hν curves for $Zn_{1-x}Fe_xO$ (x = 0, 0.01, 0.03, 0.05 & 0.07) samples.

or electron from the valence band) and the localized *d* spins on the Fe ions; (ii) The presence of small magnetic dipoles present at the surface of the nanoparticles, which interact with their nearest neighbours inside the crystals. Hence their interchange energy in these magnetic dipoles making other neighbouring dipoles to orient in that direction. As a result of which the sum of number of magnetic dipoles orienting along the unidirectional increases, as a result the ferromagnetism induces at room temperature; and the other possibility is (iii) the presence of defects induced by the incorporation of Fe into ZnO host matrix can also be the origin of the FM behavior [21–23]. The origin of observed RTFM in our Fe doped ZnO samples is attributed to any of the possibilities discussed above. But, from the XRD results, within the detection limit, no impurity phases are observed in ZnO samples doped with Fe, confirms the substitution of Fe^{2+} ions at Zn^{2+} site, forming single phase. Hence the role of impurities in the origin of ferromagnetism can be ruled out. Therefore the observed ferromagnetism in Fe doped ZnO is due to the substitution of Fe and is independent on the secondary phase of $ZnFe_2O_4$, Fe_2O_3, Fe_3O_4 and the cluster of metallic Fe.

4. Conclusions

For the first time L-Valine has been used as a fuel to synthesize nanocrystalline $Zn_{1-x}Fe_xO$ (x = 0, 0.01, 0.03, 0.05 & 0.07) particles through solution combustion technique. X-ray diffraction studies show the polycrystalline, wurtzite phase nanoparticles are formed at as-synthesized form without need of post heat treatment. No impurities of Fe oxide such as $ZnFe_2O_4$, Fe_2O_3, Fe_3O_4 were seen, which confirms that Fe is substituted at Zn site. SEM and TEM studies shows that as-synthesized samples are agglomerated, highly porous in nature and the average size of the nanoparticles is in the range of 20–30 nm. Further, the effect of Fe doping on the optical and magnetic properties were investigated. It was found that, the optical band gap energy decreases with Fe concentration due

Please cite this article in press as: N. Srinatha et al., Effect of Fe doping on the structural, optical and magnetic properties of combustion synthesized nanocrystalline ZnO particles, Advanced Powder Technology (2017), http://dx.doi.org/10.1016/j.apt.2017.01.016

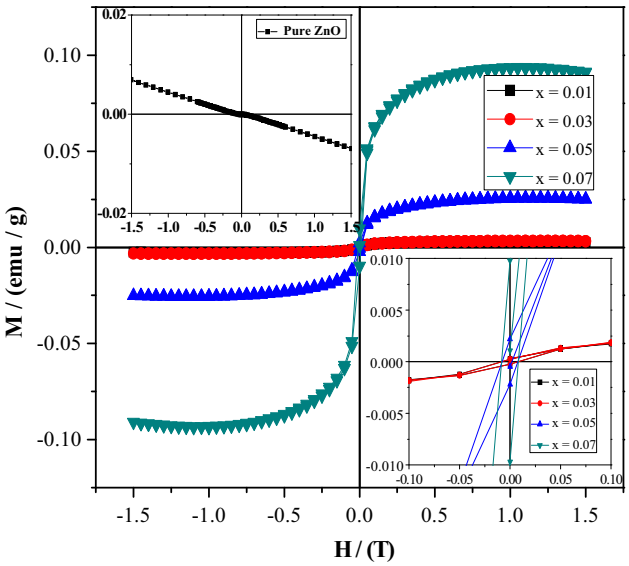

Fig. 5. Room temperature M-H plots for $Zn_{1-x}Fe_xO$ ($x = 0.01$, 0.03, 0.05 & 0.07) samples. Top-left inset is the M-H plot for $x = 0.00$ shows the diamagnetic behavior of the sample and bottom-right inset shows enlarged part hysteresis loops.

to the increase of particle size. This red shift/decrease of band gap energy was observed due to the substitution of Fe^{2+} ions at Zn^{2+} site, the formation of molecular orbitals/sub bands between the conduction band and valence band takes place and also due to the *sp – d* exchange interactions of localized Fe^{2+} electrons and valence band electrons of ZnO. Room temperature magnetic studies shows that the undoped ZnO samples exhibit diamagnetic property where as Fe doped ZnO samples exhibit RTFM with increasing coercivity with Fe concentration.

Acknowledgments

Authors (S.N and B.A) are grateful to UGC-DAE-CSR, Kalpakkam Node for the financial support through CRS No. CSR-KN/CRS-22. Authors thank Dr. P. S. Anil Kumar, Dept of Physics, IISc, Bangalore for providing SQUID facility. Authors are thankful to DST-FIST for providing XRD facilities at Department of Physics, Bangalore University, Bangalore.

References

[1] T. Dietl, H. Ohno, F. Matsukura, J. Cibert, D. Ferrand, Zener model description of ferromagnetism in zinc-blende magnetic semiconductors, Science 287 (2000) 1019.
[2] S.A. Wolf, D.D. Awschalom, R.A. Buhrman, J.M. Daughton, S. von Molnár, M.L. Roukes, A.Y. Chtchelkanova, D.M. Treger, Spintronics: a spin-based electronics vision for the future, Science 294 (2001) 1488.
[3] M. Venkatesan, C.B. Fitzgerald, J.G. Lunney, J.M.D. Coey, Anisotropic ferromagnetism in substituted zinc oxide, Phys. Rev. Lett. 93 (2004) 177206.
[4] S. Karamat, R.S. Rawat, P. Lee, T.L. Tan, R.V. Ramanujan, Structural, elemental, optical and magnetic study of Fe doped ZnO and impurity phase formation, Prog. Nat. Sci.: Mater. Int. 24 (2014) 142–149.
[5] R. Saleh, S.P. Prakoso, A. Fishli, The influence of Fe doping on the structural, magnetic and optical properties of nanocrystalline ZnO particles, J. Magn. Magn. Mater. 324 (2012) 665–670.
[6] I. Soumahoro, R. Moubah, G. Schmerber, S. Colis, M.A. Aouaj, M. Abd-lefdil, N. Hassanian, A. Berrada, A. Dinia, Structural, optical, and magnetic properties of Fe-doped ZnO films prepared by spray pyrolysis method, Thin Solid Films 518 (2010) 4593–4596.
[7] J. Kaur, R.K. Kotnala, V. Gupta, K.C. Verma, Anionic polymerization in Co and Fe doped ZnO: nanorods, magnetism and photoactivity, Curr. Appl. Phys. 14 (2014) 749–756.
[8] K.C. Patil, M.S. Hedge, T. Rattan, S.T. Aruna, Chemistry of Nanocrystalline Oxide Materials: Combustion Synthesis, Properties and Applications, World Scientific, New Jersey, 2008.
[9] J.H. Park, M.G. Kim, H.M. Jang, S. Ryu, Y.M. Kim, Co-metal clustering as the origin of ferromagnetism in Co-doped ZnO thin films, Appl. Phys. Lett. 84 (8) (2004) 1338–1340.
[10] Shuxia Guo, Zuliang Du, Influence of defects on magnetism of Co-doped ZnO, J. Magn. Magn. Mater. 324 (2012) 782–785.
[11] R. Kumar, A.P. Singh, P. Thakur, K.H. Chae, W.K. Choi, B. Angadi, S.D. Kaushik, S. Patnaik, Ferromagnetism and metal–semiconducting transition in Fe-doped ZnO thin films, J. Phys. D Appl. Phys. 41 (2008) 155002.
[12] N. Srinatha, B. Angadi, K.G.M. Nair, N.G. Deshpande, Y.C. Shao, W.-F. Pong, Spectroscopic investigation of an intrinsic room temperature ferromagnetism in Co doped ZnO nanoparticles, J. Electron. Spectrosc. Rel. Phenom. 195 (2014) 179–184.
[13] P.K. Sharma, R.K. Dutta, A.C. Pandey, S. Layek, H.C. Verma, Effect of iron doping concentration on magnetic properties of ZnO nanoparticles, J. Magn. Magn. Mater. 321 (2009) 2587–2591.
[14] G. Lawes, A.S. Risbud, A.P. Ramirez, Ram Seshadri, Absence of ferromagnetism in Co and Mn substituted polycrystalline ZnO, Phys. Rev. B 71 (2005) 045201.
[15] S. Yin, M.X. Xu, L. Yang, J.F. Liu, H. Rosner, H. Hahn, H. Gleiter, D. Schild, S. Doyle, T. Liu, T.D. Hu, E. Takayama-Muromachi, J.Z. Jiang, Absence of ferromagnetism in bulk polycrystalline $Zn_{0.9}Co_{0.1}O$, Phys. Rev. B 73 (2006) 224408.
[16] M.L. Dinesha, H.S. Jayanna, S. Mohanty, S. Ravi, Structural, electrical and magnetic properties of Co and Fe co-doped ZnO nanoparticles prepared by solution combustion method, J. Alloys Compounds 490 (2010) 618–623.
[17] B.J. Wood, R.G.J. Strens, Diffuse reflectance spectra and optical properties of some sulphides and related minerals, Mineral. Mag. 43 (1979) 509–518.
[18] R. Bhargava, P.K. Sharma, A.K. Chawla, S. Kumar, R. Chandra, A.C. Pandey, N. Kumar, Variation in structural, optical and magnetic properties of $Zn_{1-x}Cr_xO$ (x = 0.0, 0.10, 0.15, and 0.20) nanoparticles: role of dopant concentration on non-saturation of magnetization, Mater. Chem. Phys. 125 (2011) 664–671.
[19] H.V. Wenckstern, H. Schmidt, M. Brandt, A. Lajna, R. Pickenhain, M. Lorenz, M. Grundmann, D.M. Hofmann, A. Polity, B.K. Meyer, H. Saal, M. Binnewies, A. Borger, K.D. Becker, V.A. Tikhomirov, K. Jug, Anionic and cationic substitution in ZnO, Prog. Solid State Chem. 37 (2009) 153–172.
[20] S. Kumar, R. Kumar, D.P. Singh, Swift heavy ion induced modifications in cobalt doped ZnO thin films: structural and optical studies, Appl. Surf. Sci. 255 (2009) 8014–8018.
[21] X. Xu, C. Xu, J. Dai, J. Hu, F. Li, S. Zhang, Size dependence of defect-induced room temperature ferromagnetism in undoped ZnO nanoparticles, J. Phys. Chem. C 116 (15) (2012) 8813–8818.
[22] K. Sato, H. Katayama-Yoshida, Stabilization of ferromagnetic states by electron doping in Fe-, Co- or Ni- doped ZnO, Jpn. J. Appl. Phys. 40 (2001) L334.
[23] H. Gua, Y. Jiangb, M. Yana, Defect-induced room temperature ferromagnetism in Fe and Na co-doped ZnO nanoparticles, J. Alloy. Comp. 521 (2012) 90–94.